Journal of Catalysis **210,** 39–45 (2002)
doi:10.1006/jcat.2002.3638

Characterization of Boron-Nitride-Supported Pt Catalysts for the Deep Oxidation of Benzene

Chih-An Lin,* Jeffrey C. S. Wu,*,[1] Jen-Wei Pan,* and Chuin-Tih Yeh†

*Department of Chemical Engineering, National Taiwan University, Taipei, Taiwan 10617, Republic of China; and †Department of Chemistry, National Tsing-Hua University, Hsinchu, Taiwan 300, Republic of China

Received November 9, 2001; revised March 29, 2002; accepted April 11, 2002

Two kinds of hexagonal boron nitride (h-BN), with different crystallinities, were selected as supports of oxidation catalysts and compared with alumina accordingly. Platinum catalysts were prepared by the incipient wetness method with the precursor $H_2PtCl_6 \cdot 6H_2O$. Catalysts were treated at various temperatures in air or hydrogen. TEM micrographs indicate that migration of Pt particles occurred on the highly crystalline face of h-BN due to the weaker bonding between the crystalline face and Pt particles than between Pt and Pt. The grain boundary of the h-BN support with lower crystallinity strengthened bonding to Pt particles, causing the Pt particles to be well dispersed. The Pt particles dispersed on the support yielding low Pt bonding strength, such as h-BN and especially highly crystallized h-BN, were less easily oxidized. UV absorption spectra of Pt also revealed that the h-BN support can eliminate the influence of chloride from Pt particles at low temperature. Pt/h-BN is more active than Pt/γ-Al_2O_3 in benzene deep oxidation. This finding is believed to follow from Pt in the reduced state supplying more active adsorbed oxygen atoms and the lower effect of chlorine on the support. The h-BN support with low crystallinity, appropriate specific surface areas, and chemical anchoring sites is recommended as the preferred support to maintain the dispersion and activity of Pt particles.

Key Words: **hexagonal boron nitride; platinum; catalytic oxidation; benzene.**

INTRODUCTION

Supported noble metal catalysts are often used in deep oxidation of volatile organic compounds (VOCs). Materials traditionally used as supports of active phases in deep oxidation of VOCs are insulating oxides such as SiO_2, γ-Al_2O_3, silica-alumina, and various zeolites (1). The traditional supports possess low thermal conductivity and many acidic and basic sites, causing sintering of the supported metal on hot spots and coverage of the catalyst by water. Some metal–support interactions in oxidesupported metal catalysts influence catalytic activity (2). Chlorine suppresses catalytic activity of noble metals by forming oxychloride, PtO_xCl_y (3). However, many precursors of noble metals used in catalyst preparation are dissolved in hydrochloride acids.

The graphite-like hexagonal boron nitride (h-BN) is the most stable isomer of BN under ambient conditions (4). It exhibits high thermal conductivity, temperature stability, acid–base resistance, oxidation resistance, and appropriate mechanical resistance. Furthermore, h-BN is hydrophobic, preventing moisture condensation on its surface. h-BN serves well as a catalyst support in deep oxidation. However, little research has been performed in this area (5, 6).

Pt catalysts, supported on boron nitride, were recently investigated in our laboratory (5). The Pt/h-BN catalysts were compared with Pt/γ-Al_2O_3 in deep gasoline vapor oxidation. The reduced Pt/h-BN catalyst was treated with air at 300°C for 2 h before the reactions. The oxidative conversion of gasoline vapor rose to 90% at approximately 150°C. In contrast, the light-off-temperature (for 50% conversion) of Pt/γ-Al_2O_3 with the same pretreatment was 250°C. If the temperature is fixed at 185°C, the Pt/h-BN catalysts maintain their activity after 80 h, but the activity of Pt/γ-Al_2O_3 declines continuously with time. Thus, the earlier research concluded that Pt/h-BN outperforms traditional Pt/γ-Al_2O_3 with respect to the life and activity of the catalyst. This research aims to more fully characterize the surface of Pt/h-BN and to begin relating the surface structure to reactivity.

EXPERIMENTAL

(a) Preparation

Two kinds of h-BN were used as supports of catalysts. The one produced by Dojindo Co. (Japan), presumed highly crystalline, was marked "a-BN." The other, crystallized at a lower temperature than the first, from High Performance Materials Inc. (Taiwan), was marked "b-BN." Gamma alumina (γ-Al_2O_3), a commonly used support, from Merck (USA) was used as a comparison. The particle diameters of all supports were between 30 and 150 μm. Platinum catalysts with 0.37 and 3.7 wt% Pt were

[1] To whom correspondence should be addressed. Fax: 886-2-23623040. E-mail: cswu@ccms.ntu.edu.tw.

0021-9517/02 $35.00

prepared by the incipient wetness method. The precursor salt, $H_2PtCl_6 \cdot 6H_2O$, with approximately 40 wt% Pt, was purchased from Acros Organic (Belgium). Methanol from Aldrich (USA) was the diluting solvent to soak h-BN effectively. The sample was named "fresh catalyst" after drying overnight at the ambient temperature. Then, the fresh catalysts were pretreated in flowing air, at 300, 400, 500°C or in a flow of a 20% H_2/N_2 mixture at 300°C rising at 10°C/min from room temperature at 30 cm^3/min for 2 h before characterization and reaction.

(b) Characterization

The specific surface area of the supports was calculated from N_2 adsorption, using the BET equation. The hydrogen chemisorption equipment and the determination of platinum dispersion were similar to those described by Yang and Goodwin (7). TEM (Hitachi H-7100 Transmission Electron Microscope) was employed to observe the shape of h-BN and the appearance of Pt particles dispersed on h-BN. The LEED (low-energy electron diffraction) patterns of h-BN were detected by the Hitachi S-800 Field Emission device. The crystalline phase of h-BN was examined by X-ray diffraction (XRD). The XRD equipment of type M03XHF22 from the Material Analysis and Characterization Company was operated at 40 kV, with a 1.54056 Å X-ray wavelength from a Cu target and a scanning speed of 0.5 degree/min.

The precise Pt loading of the catalysts was measured by the wet chemical method. The catalysts were immersed in HF for more than 2 days to dissolve platinum from the surface. The solution was filtered and diluted with deionized water to the appropriate concentration. A series of standard Pt solutions (Aldrich) were used to yield calibration curves. The Pt concentrations of solutions were determined with a transmission UV absorption wavelength of 261.8 nm (8).

Figure 1 shows the TPR equipment used in this study. The thermal conductive detector was made by China Chromatography (Taiwan). The gas used in TPR was a mixture of 5 vol% H_2 in Ar and the oxidizing gas was air. The procedure involved the following steps: (1) The fresh catalyst, reduced in a 20% H_2/N_2 mixture, was oxidized in air for 2 h at 300°C, cooled in air to the ambient temperature, and cooled continuously to −90°C in N_2. The carrier gas was changed from N_2 to the H_2/Ar mixture, when stable signals were obtained. (2) Thereafter, TPR was conducted in the H_2/Ar mixture, up to 600°C at a constant heating rate of 7°C/min.

XPS (X-ray photoelectron spectroscopy) was measured by a VG MICROTECH MT-500 machine with a Mg target. The C 1s signal at 284.6 eV was taken as the standard to correct the binding energy. The $4f_{7/2}$ binding energy of platinum was measured to examine the state of platinum particles dispersed on the support. The 1s binding energy

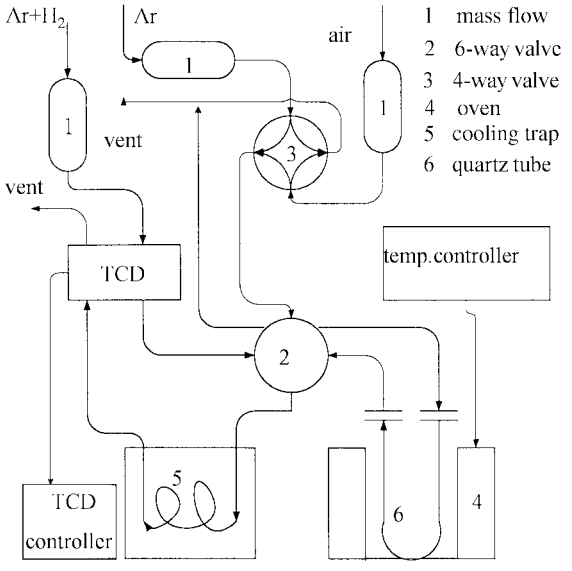

FIG. 1. TPR apparatus.

of boron was considered to survey the surface chemical species of the h-BN support.

Reflective UV–vis measurement was conducted by a Hitachi U-3410 spectrophotometer. The scanning range was between 200 and 800 nm. The reflective UV–vis spectra were used to confirm the states of platinum on the catalyst containing only 0.37 wt% Pt, due to the low sensitivity of XPS (more than 0.3% (9)).

(c) Catalytic Oxidation

Catalytic activity was examined by the deep oxidation of benzene. Benzene was purchased from Alps (USA). The reactor system in this research was the same as in the literature (5). An air stream through a saturator filled with benzene mixed with a bypass air stream. The concentration of benzene in the feed was approximately 600 ppmv. The mixture passed through the reactor at a rate of 150 ml/min, around 21,000 h^{-1} (VHSV). The reactor contained 0.3 g of catalyst in each reaction. The reaction temperature rises from 100 to 300°C. The concentration of benzene was measured at least two or three times in the steady state at each temperature using an HP GC6890, with thermal conductive and flaming ion detectors connected in series. The reaction was also carried out under various flow rates to check the effect of mass-transfer resistance on the catalyst. No significant activity change was found, i.e., mass-transfer resistance can be ruled out.

RESULTS AND DISCUSSION

Table 1 lists the specific surface areas of the supports, measured by N_2 adsorption and calculated from the BET method. γ-Al_2O_3 exhibits the largest specific surface area of the three supports at 100 m^2/g. The specific surface area

TABLE 1

The Specific Surface Area of the Support

Support	Specific surface areas (m^2/g)
Al_2O_3	100
b-BN	30
a-BN	2

of a-BN is 2 m^2/g and that of b-BN is 30 m^2/g. The specific surface areas, after the reactions with benzene or air treatment at 500°C for 2 h, are similar to those obtained without any thermal treatment. The Pt dispersion measured by hydrogen chemisorption, given in Table 2, increases with the specific surface area of the support. The Pt/γ-Al_2O_3 catalyst shows a Pt dispersion around 30%. Pt/a-BN and Pt/b-BN, with lower specific surface areas of their supports, give lower dispersions. The dispersion of the two Pt/b-BN catalysts is around 20% and that of the 0.37 wt% Pt/a-BN catalyst approaches 10%. However, the dispersion of Pt/a-BN declines drastically to 1% when the Pt loading increases to 3.7 wt%, showing that the Pt loading of 3.7 wt% exceeds the capacity of the surface area of a-BN for high dispersion. The average diameter of Pt particles can be calculated from an experimentally determined equation in which the product of the dispersion and the particle diameter is near 1.1 (8, 10, 11). Table 2 also shows the average diameter of Pt particles. Most platinum particle sizes are between 3 and 10 nm, except those of 3.7 wt% Pt/a-BN, which exceed 100 nm.

Figure 2 shows the LEED patterns of h-BN to clarify the long-range order of the surface species. The pattern of a-BN in Fig. 2a reveals a hexagonal structure with sharp spots. In contrast, the LEED pattern for b-BN, in Fig. 2b, reveals spots which are split by the constructive and destructive interference due to multiple domains, suggesting the presence of a more amorphous surface structure. The h-BN crystal can be confirmed by observing the XRD signals. The peaks at 26.8, 41.6, 43.8, 50.1, and 55.2° belonging to hexagonal h-BN can be observed in the spectra of a-BN and b-BN. The size of the crystal domain is determined by XRD, using the Scherrer equation. The crystal size of a-BN is 53 nm and the crystal size of b-BN is 35 nm, consistent with the observed LEED patterns.

TABLE 2

Dispersion and Pt Particle Diameter of Catalysts

Catalysts	Dispersion (%)	Pt particle diameter (nm)[a]
0.37% Pt/Al_2O_3	29	3.6
0.37% Pt/b-BN	19	5.7
0.37% Pt/a-BN	10	11
3.7% Pt/b-BN	18	6.1
3.7% Pt/a-BN	1	110

[a] The Pt particle diameter is calculated from the experimentally determined equation: Dispersion × particle diameter (nm) = 1.1 (8, 10, 11).

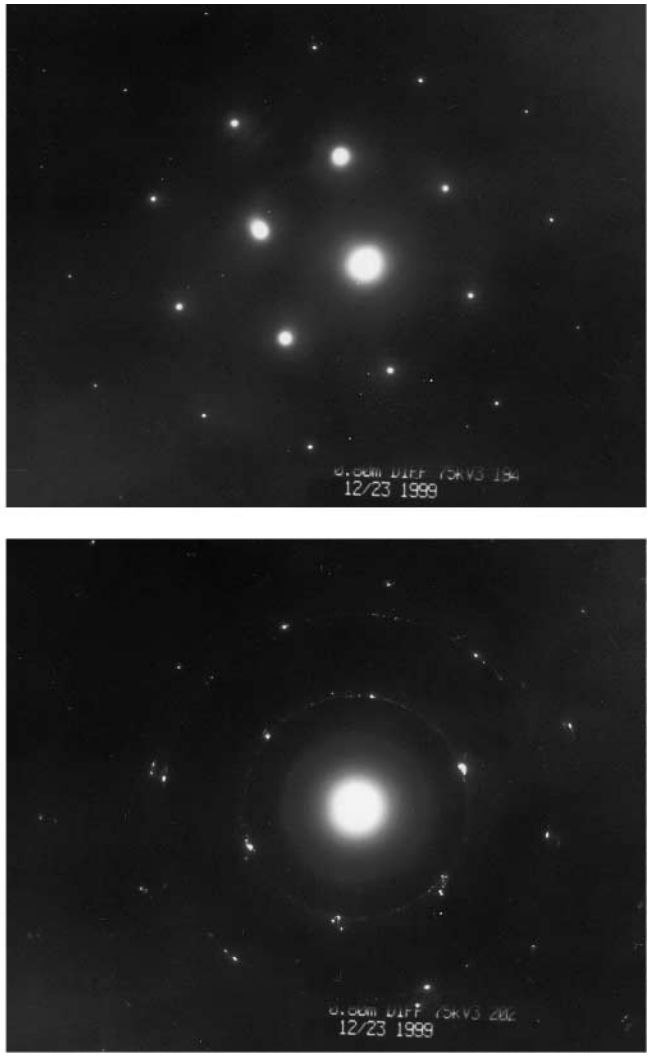

FIG. 2. The LEED patterns of h-BN: (a) a-BN; (b) b-BN.

Figure 3 presents TEM images of Pt/h-BN following reduction by an H_2/N_2 mixture at 300°C. The catalyst surfaces are observed at a magnification factor of 100,000. In Figs. 3a and 3b, the surface of b-BN is clearly less ordered than that of a-BN. The platinum particle diameter of 0.37 wt% Pt/b-BN in Fig. 3a is close to that calculated from the dispersion. The Pt particles remain well dispersed after reduction at 300°C. However, three kinds of dispersed Pt particles can be found on 0.37 wt% Pt/a-BN in Fig. 3b. The first kind of Pt particle, with a diameter under 10 nm, falls in line on the edge of the crystal face. The second type of Pt particle is triangular, with a diameter between 10 and 30 nm, and is located at the center of an a-BN crystal face. The triangular particles are thought to be formed by the migration and crystallization of smaller Pt particles, when the surface is reduced by an H_2/N_2 mixture at 300°C. The third kind of Pt particle is sometimes triangular and has the largest diameters, between 30 and 90 nm. Reduction at 300°C cannot

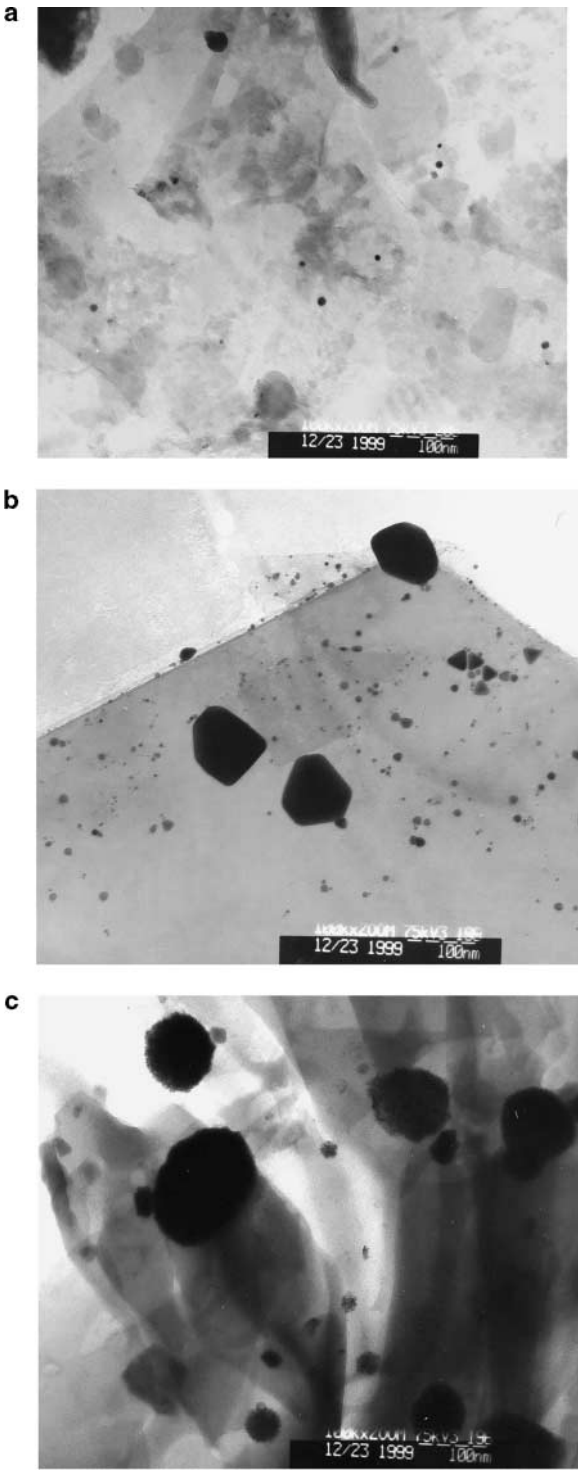

FIG. 3. The TEM micrographs of catalysts (a) 0.37 wt% Pt/b-BN, (b) 0.37 wt% Pt/a-BN, and (c) 3.7 wt% Pt/a-BN.

decompose the large clusters of Pt precursors but can recrystallize them. The triangular shape of the Pt particles follows from a minimization of the surface free energy by the fcc metal, implying that the interaction between Pt particles and the a-BN surface is weaker than the Pt–Pt interaction.

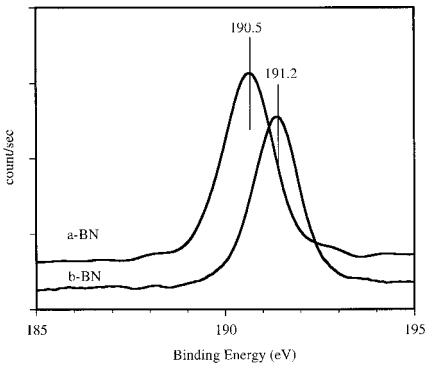

FIG. 4. XPS of Boron 1s of two h-BNs.

The TEM image of 3.7 wt% Pt/b-BN is similar to that of 0.37 wt% Pt/b-BN. However, the TEM image of 3.7 wt% Pt/a-BN in Fig. 3c reveals that most Pt particles exist as the largest kind. Such particles are assumed to form when Pt precursors are deposited on the surface and exceed the capacity of the surface area of a-BN to disperse the Pt.

Figure 4 shows the B 1s binding energies of two kinds of h-BNs, determined by XPS. Two kinds of h-BNs, following treatment with air at 500°C, exhibit the same B 1s binding energies as those without any thermal treatment, revealing the high thermal stability of h-BN. Signals at 190.5 eV in a-BN's spectrum and at 191.2 eV in b-BN's spectrum can be observed. These binding energies are shifted from the standard B–N binding energy found in an XPS handbook of 190.3 eV (12). The shift is believed to follow from B–O bonding within the BN crystal (13). The greater shift of b-BN suggests greater B–O bonding. The structure of hexagonal BN, presented in Fig. 5, implies that the edge of an h-BN crystal may contain B–O bonding. The higher crystallization of a-BN may reduce the amount of B–O bonding. The structure of h-BN and the TEM images suggest that B–O bonding can assert a bonding strength to platinum particles on h-BN, whereas the crystal face of h-BN cannot. This may be why Pt particles dispersed on b-BN possess a greater bonding strength than those dispersed on a-BN. The traditional γ-Al_2O_3 support is thought to most strongly bond to Pt particles, followed by b-BN, and then a-BN. More acidic and basic sites are located on the surface

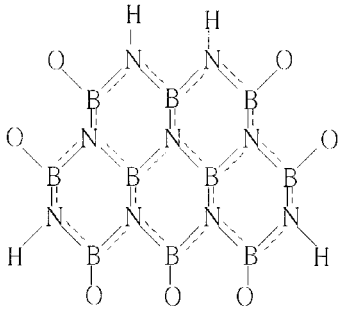

FIG. 5. The surface structure of h-BN.

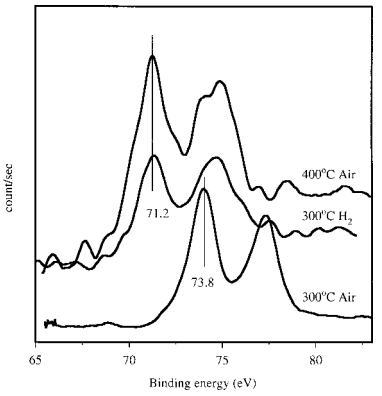

FIG. 6. XPS of Pt 4f of 3.7 wt% Pt/a-BN under various pretreatments.

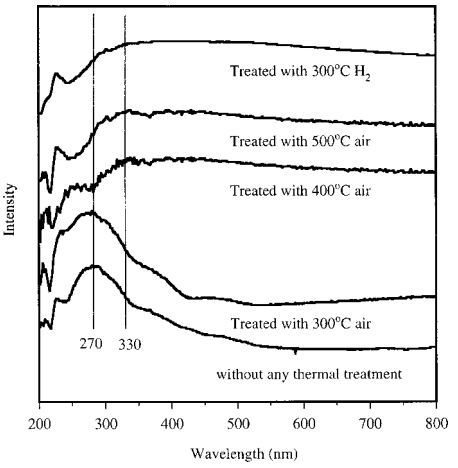

FIG. 7. Reflective UV–vis spectra of 3.7 wt% Pt/a-BN under various treatments.

of γ-Al_2O_3 than on the surface of h-BN. Consequently, Pt particles can be efficiently dispersed on γ-Al_2O_3. The lower bonding strength between Pt particles and the h-BN support yields lower Pt dispersion and larger Pt particles (14). However, the Pt loading of Pt/h-BN inspection reveals no obvious Pt loss following reaction and high-temperature treatment. The weak bonding strength between the support and Pt particles on Pt/h-BN suffices to fasten dispersed Pt particles on the surface.

Figure 6 shows the Pt $4f_{7/2}$ binding energies on 3.7 wt% Pt/a-BN with various pretreatments, obtained by XPS. Hydrogen pretreatment at 300°C and air treatment at 400°C both yield a binding energy of 71.2 eV. In contrast, air pretreatment at 300°C gives a binding energy of 72.3 eV, compared to the standard binding energy of Pt $4f_{7/2}$ in the metal state at 70.8 eV (12). The shift from 70.8 to 72.3 eV is presumed to be due to the existence of a PtO_xCl_y complex on the a-BN surface, because the Pt precursors contain chloride. The catalyst treated with an H_2/N_2 mixture at 300°C is considered reduced. However, Hwang and Yeh (15, 16) suggest that the oxygen chemisorption on Pt particles can reoccur under ambient conditions, even following reduction at high temperature. Thus, the shift from 70.8 to 71.2 eV in the spectrum of 3.7 wt% Pt/a-BN with hydrogen pretreatment at 300°C is believed to follow from the formation of weak surface Pt–O bonding on the Pt particles. Interestingly, air pretreatment at 400°C gives the same Pt $4f_{7/2}$ binding energy as hydrogen pretreatment at 300°C. The Pt precursor is suggested to be decomposed in air at 400°C and chlorine is thought to be emitted from the cluster of Pt precursors. Accordingly, the chemical species of Pt particles in 3.7 wt% Pt/a-BN with air treatment at 400°C are the same as those under hydrogen pretreatment at 300°C.

Figure 7 shows the reflective UV–vis spectra of 3.7 wt% Pt/a-BN. The absorption band near 270 nm can be observed both before and after treatment with air at 300°C. Another absorption band around 330 nm can be observed in the spectra of this catalyst with air pretreatment above 400°C, or with hydrogen treatment at 300°C. Lietz *et al.* (17) suggest that the absorption band of Pt at 262 nm corresponds to an electron transfer from chlorine to platinum, resulting in a shift to wavelengths higher than those of the Pt–Cl band. This shift is thought to be due to presence of a PtO_xCl_y complex. The wavelength of the absorption band, between 310 and 400 nm, demonstrates the existence of Pt in metal or oxide states. Accordingly, the surface of this catalyst following air pretreatment at 300°C has a residue of Pt chloride. In contrast, the UV absorption band of Pt–Cl cannot be observed on this catalyst with air treatment at above 400°C or with hydrogen treatment at 300°C, consistent with the Pt $4f_{7/2}$ binding energy (Fig. 6). Applying the measurement of reflective UV–vis absorption spectra to characterize other catalysts reveals an absorption band at 270 nm in the spectra of Pt/γ-Al_2O_3 with all pretreatments and of Pt/b-BN with treatment in air at 300°C, implying the presence of a PtO_xCl_y surface complex. In contrast, the band around 270 nm is absent from the spectrum of 0.37 wt% Pt/a-BN following air treatment at 300°C, implying that air treatment more easily removes the surface chloride complex from the catalyst supported by a-BN with low Pt loading.

Figure 8 displays the TPR spectra. Catalysts containing 0.37 wt% Pt are reduced in a hydrogen and nitrogen mixture

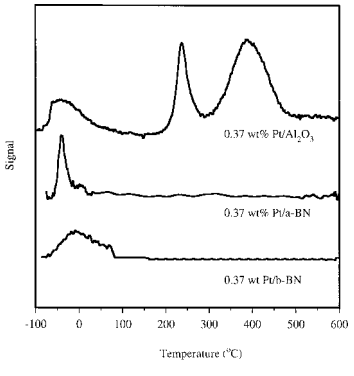

FIG. 8. TPR spectra of 0.37 wt% Pt catalysts.

and calcined in air at 300°C for 2 h before the TPR experiment. Hwang and Yeh (15, 16) suggest that the peaks between 300 and 400°C, near 200°C, near 100°C, near 50°C, and under 0°C correspond to the reduction of a PtO_xCl_y complex, the reduction of Pt-aluminate, the reduction of PtO_2, the reduction of PtO, and weak surface Pt–O bonding, respectively. The TPR spectra presented here reveal signals of the PtO_xCl_y complex, Pt-aluminate, and the combined signal of PtO_2, PtO, and weak surface Pt–O bonding in the Pt/γ-Al_2O_3 spectrum. However, signals below 100°C are observed in the Pt/b-BN spectrum and signals below 0°C are observed only in the Pt/a-BN spectrum, revealing that Pt particles dispersed on h-BN can be reduced more easily than those dispersed on γ-Al_2O_3. Consequently, the oxygen atom adsorbed on the Pt atom dispersed on h-BN is more active than those adsorbed on Pt/γ-Al_2O_3. Baumer and Freund postulate (14) that the interaction between the latter transition metal and the oxide support frequently causes electron deficiency in the metal. In this work, the weak bonding strength of Pt to h-BN reduces the electron deficiency on Pt. The combined results of characterization reveal that Pt particles can remain in the reduced state more easily when the support more weakly bonds to Pt particles, as in the case of h-BN-supported Pt, but in contrast to the case with γ-Al_2O_3.

After the Pt/h-BN catalysts are characterized, their capacities for oxidation are tested. The effect of mass transfer can be excluded because the activity (as measured by turnover frequency, TOF) did not vary when we changed the flow rates at the same temperature during reaction. Figure 9 illustrates the application of Pt catalysts to benzene oxidation. The conversion and TOF against temperature curves of catalysts supported by h-BN are steeper than those of catalysts supported by γ-Al_2O_3. This result follows from the uniform activity of Pt particles dispersed on h-BN. The surface of h-BN is much barer than that of γ-Al_2O_3, owing to the few acidic and basic sites. Therefore, Pt particles dispersed on h-BN give uniform activity.

The light-off temperatures of Pt/h-BN, shown in Figs. 9b and 9c, are between 140 and 170°C. In contrast, those of Pt/γ-Al_2O_3, shown in Fig. 9a, are from 170 to 240°C. Obviously, Pt/h-BN can be activated at lower temperature than Pt/γ-Al_2O_3. The TOF of benzene oxidation also shows a similar conversion trend. The TOF of 0.37 wt% Pt/a-BN, shown in Fig. 9c, is almost twice those of other catalysts. Such high TOF is due to the low Pt dispersion on 0.37 wt% Pt/a-BN (see Table 2) because the conversion of benzene oxidation would not be influenced by the Pt dispersion (18).

Volter *et al.* (3) and Aryafar and Zaera (19) both conclude that hydrocarbon oxidation reactions over platinum occur on reduced sites more easily than on oxidized sites. Hence, Pt particles on Pt/h-BN are more easily maintained in their reduced state, as determined in the earlier characterization, a result which is believed to be the most important in causing the difference between the activities. Barresi and Baldi (20, 21) suggested that the deep oxidation of benzene proceeds by a simplified Langmuir–Hinshelwood mechanism and that the rate of oxygen adsorption is much lower than the rate of benzene adsorption. Thus, oxygen adsorption is the rate-determining step in this reaction. Weaker bonding between platinum and oxygen on Pt/h-BN, as indicated by the TPR spectra, is thought to be responsible for supplying the more reactive surface oxygen atoms in the deep oxidation of benzene. The lower activity of Pt/γ-Al_2O_3 is believed to be due to strong bonding between Pt and O and the presence of more residual PtO_xCl_y complex on the surface of the support.

Figure 9b indicates that 0.37 wt% Pt/b-BN treated with air at 400° or 500°C, or H_2 at 300°C, was notably more active than 0.37 wt% Pt/b-BN with air treatment at 300°C,

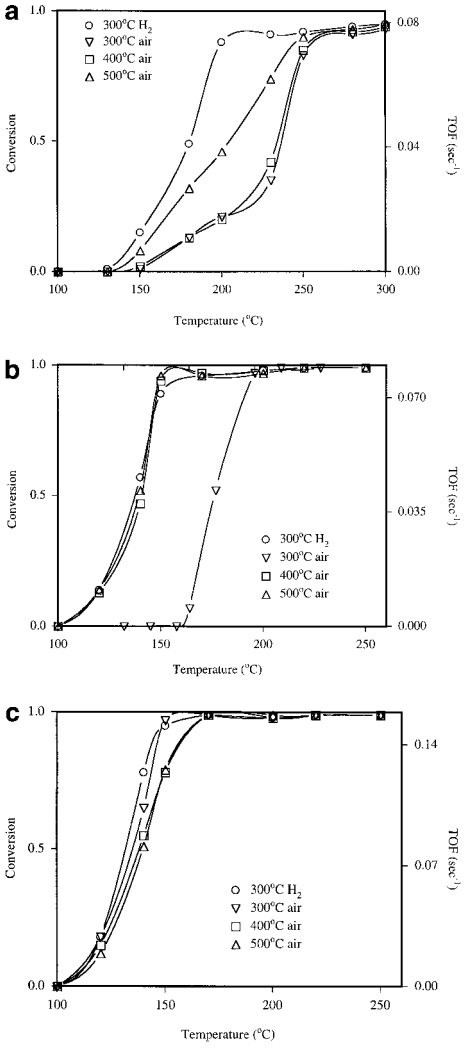

FIG. 9. The conversions and TOFs of 640 ppmv benzene oxidation on catalysts under various pretreatments: (a) 0.37 wt% Pt/Al_2O_3; (b) 0.37 wt% Pt/b-BN; and (c) 0.37 wt% Pt/a-BN.

resulting in a lower light-off temperature of around 140°C. Similar results are obtained using 3.7 wt% Pt/b-BN or 3.7 wt% Pt/a-BN with various pretreatments. Pt precursors may still be present on the surface, following air treatment at 300°C, as shown earlier by the UV–vis adsorption spectra. Pt–Cl bonding deactivates the oxygen atom adsorbed on the surface of Pt particles, probably causing the difference in activity.

Figure 9c presents the result of applying 0.37 wt% Pt/a-BN, with various pretreatments, to benzene oxidation. The reactivity of 0.37 wt% Pt/a-BN with air treatment at 300°C is similar to that of this catalyst with other pretreatments but contrasts with the 300°C air-treated 0.37 wt% Pt/b-BN catalyst, which is less reactive. The existence of Pt–Cl is not revealed by the UV–vis adsorption spectra of 0.37 wt% Pt/a-BN with air pretreatment at 300°C. Thus, the absence of Pt–Cl is suggested to be the cause of the higher activity of 0.37 wt% Pt/a-BN with air pretreatment at 300°C. The differences among the activities of the catalysts imply that the catalysts are more easily reducible on a-BN than on b-BN, consistent with the characterization by TPR and UV–vis spectroscopy.

CONCLUSION

Crystal faces of h-BN bond more weakly to Pt particles than do grain boundaries, as observed in the TEM images. Accordingly, h-BN, with higher crystallinity, exhibits a lower bonding strength to Pt overall. The surface of h-BN generally bonds more weakly to Pt particles than does γ-Al_2O_3. This weaker bonding between the support and the Pt particles allows the particles more easily to remain in reduced states. The reduced states of Pt particles on Pt/h-BN causes a weaker Pt–O bond on the surface of Pt particles to supply more reactive oxygen atoms and thus promote benzene oxidation. Therefore, the Pt/h-BN catalyst is suggested to apply to the oxidation reaction whose rate-determining step is the activation of the oxygen. Although the catalyst with low Pt loading, dispersed on a-BN, shows the greatest activity in benzene oxidation, b-BN, with a lower crystallinity and a higher specific surface area than a-BN, is recommended as the most appropriate support.

ACKNOWLEDGMENTS

The authors thank the National Science Council of the Republic of China for financially supporting this research under Contract NSC 89-CPC-7-002-014 and NSC 89-2214-E-002-065.

REFERENCES

1. Spivey, J. J., *Ind. Eng. Chem. Res.* **26**, 2165 (1987).
2. Yao, H. C., Sieg, M., and Plummer, H. K., Jr., *J. Catal.* **59**, 365 (1979).
3. Volter, J., Lietz, G., Spindler, H., and Lieske, H., *J. Catal.* **104**, 375 (1987).
4. Alkoy, S., Toy, C., Gonul, T., and Tekin, A., *J. Eur. Ceram. Soc.* **17**, 1415 (1997).
5. Wu, J. C. S., Lin, Z.-A., Pan, J.-W., and Rei, M.-H., *Appl. Catal. A* **219**, 117 (2001).
6. Jacobsen, C. J. H., *J. Catal.* **200**, 1 (2001).
7. Yang, C.-H., and Goodwin, J. G., Jr., *J. Catal.* **78**, 182 (1982).
8. Burguete, C. P., Solano, A. L., and Reiniso, F. R., *J. Catal.* **128**, 397 (1991).
9. Birggs, D., and Seah, M. P., "Practical Surface Analysis, Volume 1—Auger and X-Ray Photoelectron Spectroscopy," 2nd ed., p. 15, Wiley, New York, 1990.
10. Masayoshi, K., Yasunobn, I., Nobuo, T., Robert, L. B., John, B. B., and Jerome, B. C., *J. Catal.* **64**, 74 (1980).
11. O'Leary, D. J., Loffler, D. G., and Boudart, M., *J. Catal.* **121**, 131 (1990).
12. Moulder, J. F., Stickle, W. F., Sobol, P. E., and Bombem, K. D., "Handbook of X-Ray Photoelectron Spectroscopy," Physical Electronic Inc., Eden Prairie, MN, 1995.
13. Rudolph, S., *Am. Ceram. Soc. Bull.* **79**(6), 50 (2000).
14. Baumer, M., and Freund, H.-J., *Prog. Surf. Sci.* **61**, 127 (1999).
15. Hwang, C.-P., and Yeh, C.-T., *J. Mol. Catal. A: Chem.* **112**, 295 (1996).
16. Hwang, C.-P., and Yeh, C.-T., *J. Catal.* **182**, 48 (1999).
17. Lietz, G., Lieske, H., Spindler, H., Hanke, W., and Volter, J., *J. Catal.* **81**, 17 (1983).
18. Carballo, L. M., and Wolf, E. E., *J. Catal.* **53**, 366 (1978).
19. Aryafar, M., and Zaera, F., *Catal. Lett.* **48**, 173 (1997).
20. Barresi, A. A., and Baldi, G., *Ind. Eng. Chem. Res.* **33**, 2964 (1994).
21. Barresi, A. A., and Baldi, G., *Chem. Eng. Sci.* **47**, 1943 (1992).